Lecture 14

Some typical XPS studies

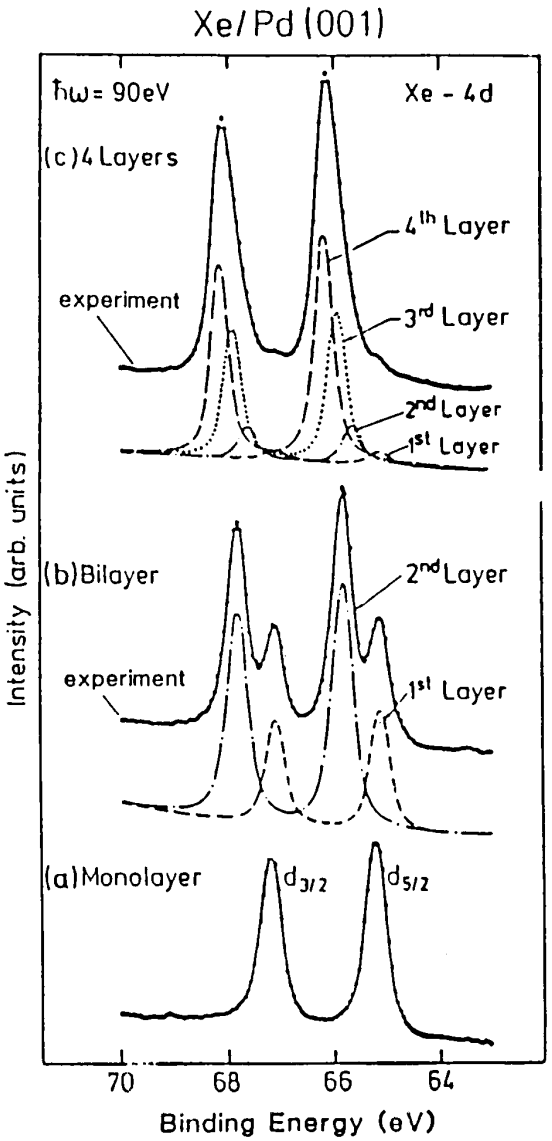

Fig.2.34. Xe 4d core-level PE spectra for (a) a monolayer, (b) a bilayer and (c) four layers of Xe on Pd(001). The binding energies are with respect to the vacuum level of the adsorbate covered substrate. The solid curves are the result of a least-squares fit of the experimental data (full dots) to (a) one spectrum, (b) two spectra (1st and 2nd layer) and (c) 4 spectra (1st to 4th layer) [2.76]

Photoelectron spectroscopy is surface sensitive, to the extent that it can distinguish monolayers. It is also possible to distinguish one layer from the next layer, etc.

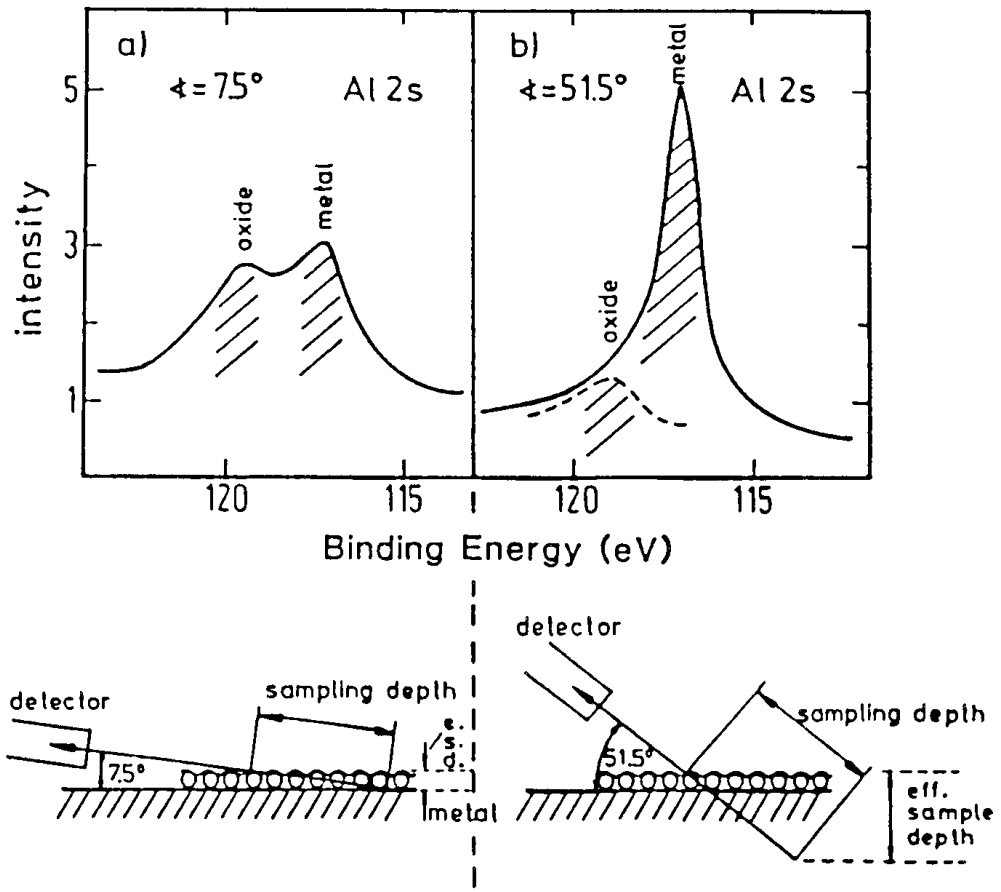

Fig.2.32. Surface sensitivity of XPS, demonstrated by changing the electron detection angle relative to the surface for a slightly oxidized surface of Al. At 7.5°, the Al 2s signals from Al metal and oxidized Al have the same magnitude, while at 51.5° the oxide signal is hardly visible [2.74]

Surface sensitivity enhancement is possible by tilting the sample.

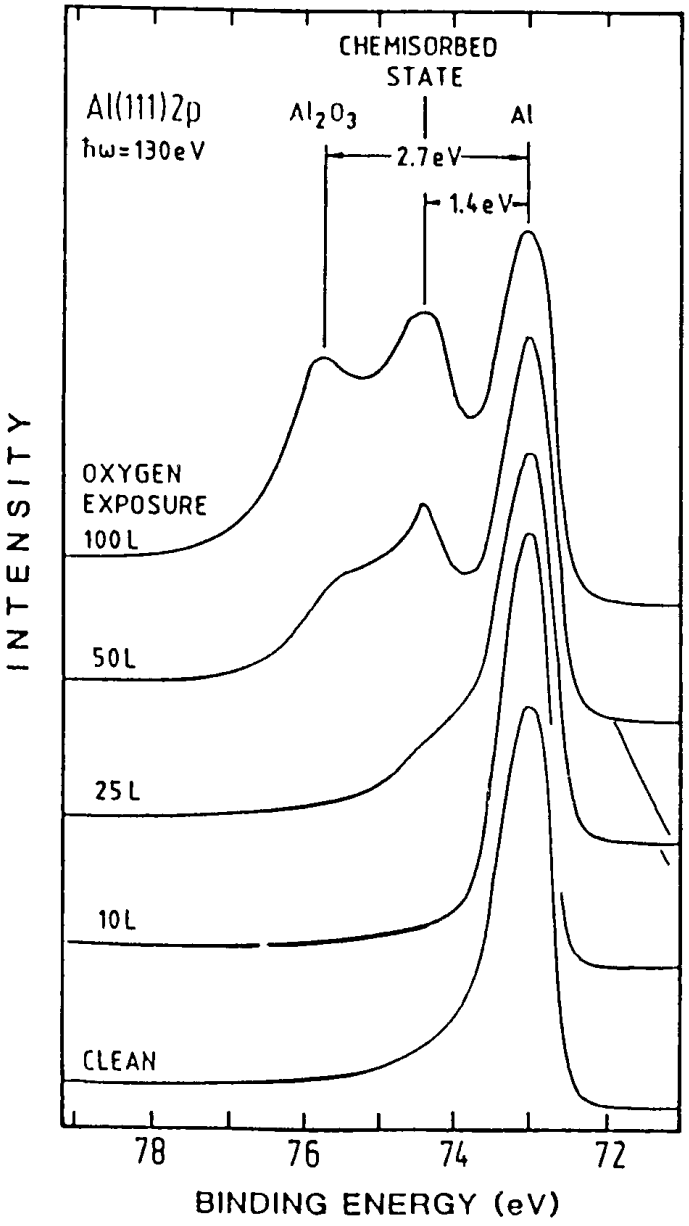

Fig.2.33. Oxidation of a (111) surface of Al monitored via the Al 2p level with $\hbar\omega$ = 130 eV synchrotron radiation [2.75]. The development of a chemisorbed state and subsequent oxide formation can be observed

We can study evolution of surface species. This helps us to understand the origin of reactivity.

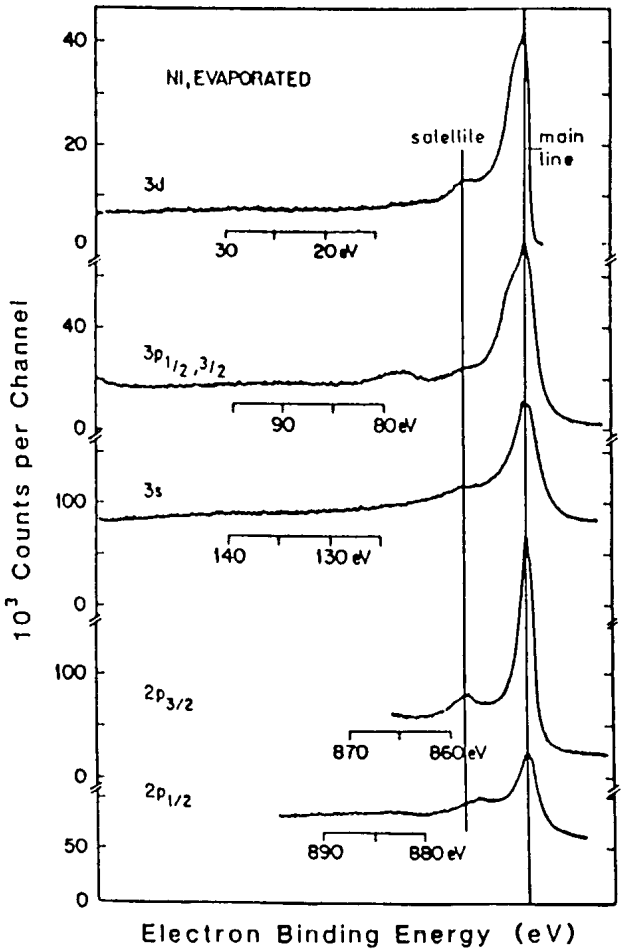

Fig.3.13. XPS spectra of the 3d, 3p, 3s, $2p_{3/2}$ and $2p_{1/2}$ levels of Ni metal [3.10]. The main lines have been lined up to demonstrate the constant distance of the satellite position (even for the 3d valence band)

The difference between the main line and the satellite is the same for several core holes indicating that the configurations are the same.

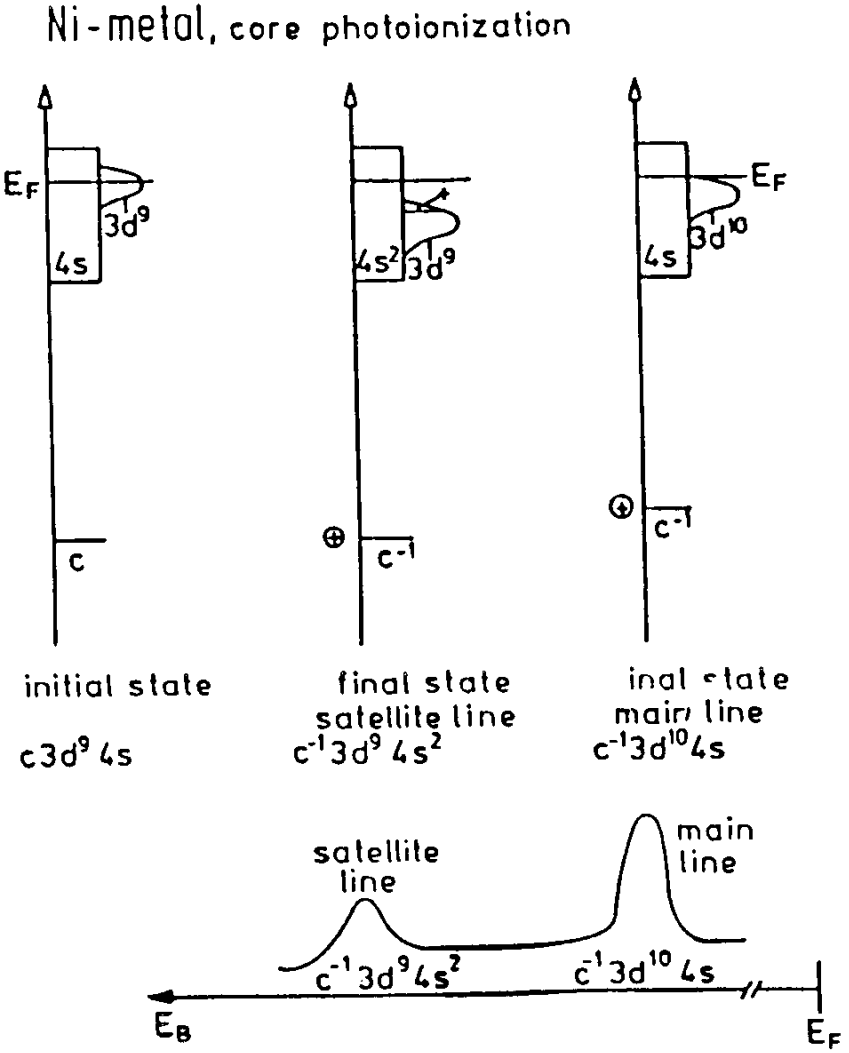

This is explained schematically here.

Fig.3.14. Schematic density of states of Ni, indicating the origin of the main line and the satellite for core ionization (c^{-1}); for valence band ionization see also Fig.3.19. The initial state is $c3d^9 4s$ and the two final states are $c^{-1}3d^9 4s^2$ (satellite) and $c^{-1}3d^{10}4s$ (main line); c denotes a core level, c^{-1} a core hole

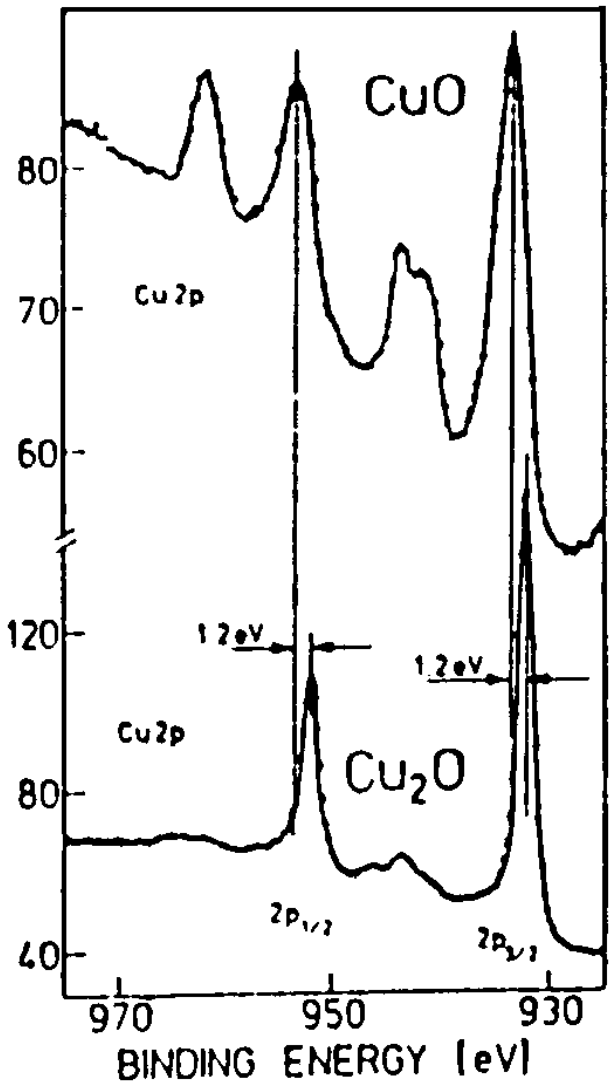

Satellite can be used to distinguish oxidation state.

Fig. 3.2. XPS spectrum of the Cu $2p_{1/2}$–$2p_{3/2}$ core levels in Cu_2O (bottom) with a d^{10} configuration and CuO (top) with a d^9 configuration [3.32]. The CuO spectrum shows strong satellites

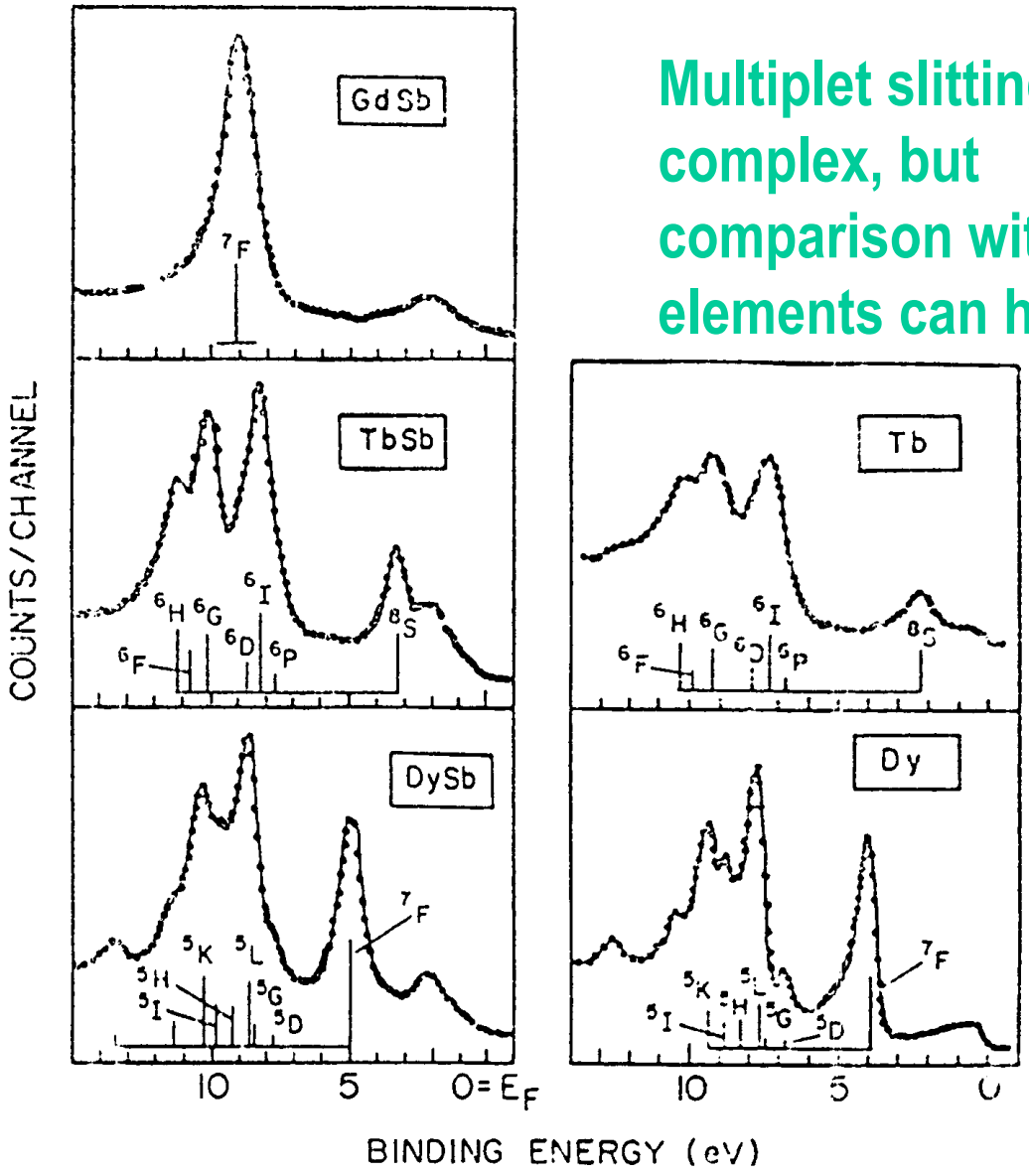

Fig. 4. (b) GdSb, TbSb and Tb, and DySb and Dy.

Multiplet slitting can be complex, but comparison with the elements can help.

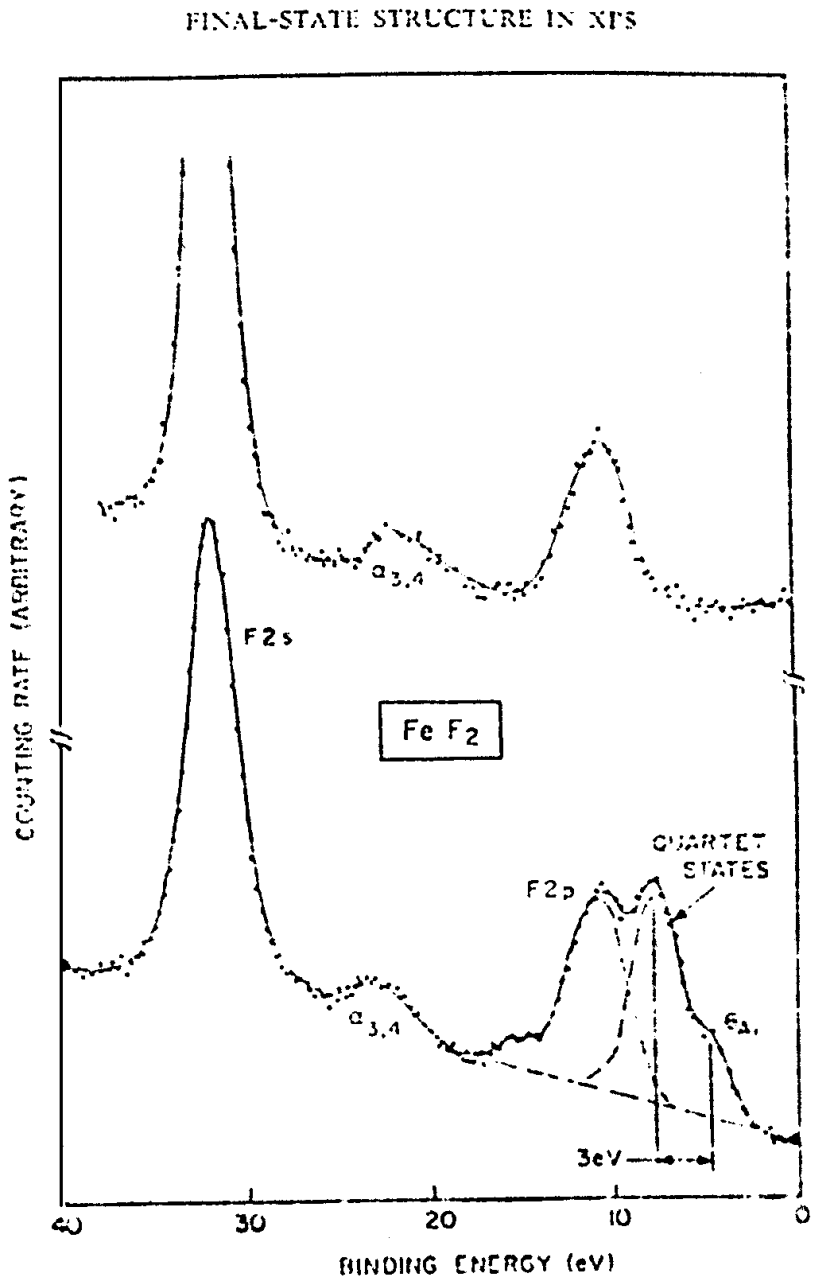

g. 7. Valence-band spectrum of FeF2 and LiF (after Wertheim *et al.*[25]).

Multiplet can arise in the xps valence band of simple solids

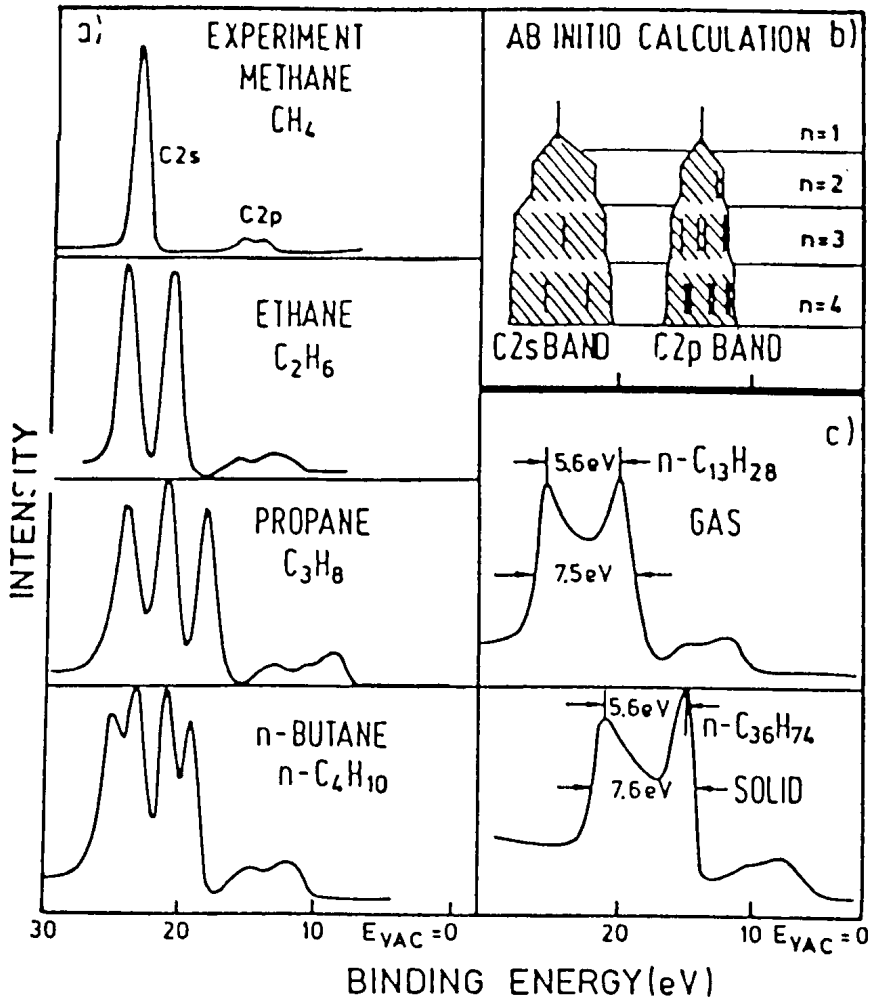

Fig.5.20. (a) EDCs of a number of linear polymers [5.30]: CH_4, C_2H_6, C_3H_8 and C_4H_{10}; (b) comparison with the ab initio calculation of their valence bands. The C 2s orbital nicely shows the splitting expected into 1, 2, 3 and 4 levels. (c) For higher members of this family the single orbitals originating from the C 2s level can no longer be resolved and lead to a structure seen e.g. in the gas phase spectrum of $C_{13}H_{28}$. This spectrum is very similar to the one observed in solid samples such as $C_{36}H_7$

Evolution of band structure

CH_4 $(1s\ a_1)^2$ $(2s\ a_1)^2$ $(2p\ t_2)^6$

C_2H_6 $(1a_2n)^2$ $(1a_1g)^2$ $(2a_1g)^2$ $(2a_2n)^2$ $(1e_n)^4$ $(3a_1g)^2$ $(1e_g)^4$/2p

You can see the orbitals clearly in UPS

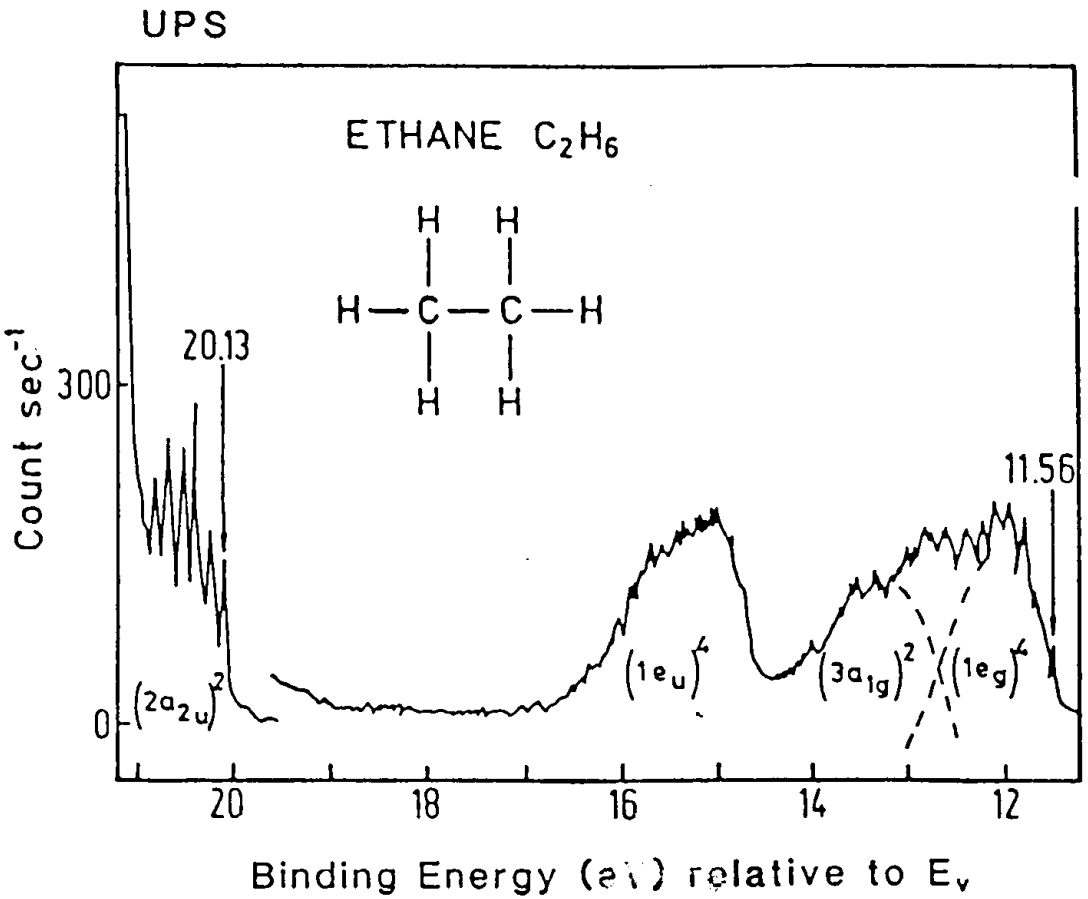

Fig.5.21. UPS (21.2eV) spectrum of C_2H_6 to study the structure in the 2p-derived orbitals [5.1]. The three expected orbit[illegible]an barely be discerned